# Interference Analysis of Anti Micro and Small Unmanned Aircraft Systems and Code Division Multiple Access Systems at Frequency Band 835–845 MHz

Junfang Li[1], Changqing Zhang[2(✉)], Jie Liu[3], Yangmei Zhang[1], Kun Liu[1], and Fei Song[1]

[1] School of Electronic Engineering, Xi'an Aeronautical University, Xi'an 710077, China
lijf@aliyun.com, 201707019@xaau.edu.cn
[2] College of Information Engineering,
Xinyang Agriculture and Forestry University, Xinyang 464000, Henan, China
[3] Xi'an Branch, China Academy of Space Technology, Xi'an 710100, China

**Abstract.** An anti micro and small unmanned aircraft system (AmsUAS) is a radio technology used for civil micro and small unmanned aircraft systems (msUASs) control. Along with blocking the communication link of the msUAS, the AmsUAS also interferes with other radio communication systems such as civil aviation and mobile communication systems. In this study, an analysis method based on the interference-to-noise ratio (INR) criterion is proposed and interference analysis is performed on AmsUAS and code division multiple access (CDMA) systems. First, to control msUASs, it is necessary to calculate the minimum transmit power of the AmsUAS in the corresponding frequency band according to the uplink and the radio wave propagation distance of the msUAS. Second, to avoid harmful interference to other radio systems (such as CDMA), the frequency and distance separation between the AmsUAS and CDMA radio systems should be calculated according to factors such as application scenarios, radio wave propagation distance, and working frequency band. Finally, a simulation analysis provides the transmit power, off-axis angle, frequency separation, and distance separation of the AmsUAS and CDMA systems in different environments.

**Keywords:** Anti micro and small unmanned aircraft system · Code division multiple access · Interference analysis · Interference-to-noise ratio criterion

## 1 Introduction

With the development of civil unmanned aircraft systems, micro and small unmanned aircraft systems (msUASs) have been widely used in various fields [1–3]. With their low cost, low volume, and light weight, msUASs can perform remote operations conveniently, acquire high-resolution images, access hard-to-reach areas, and obtain flexible response to complex geographical environments. Owing to such advantages, msUASs


X. Wang et al. (Eds.): AICON 2021, LNICST 396, pp. 469–482, 2021.
https://doi.org/10.1007/978-3-030-90196-7_40

are widely used in aviation filming [4], infrastructure detection monitoring [5], accident scene investigation [6], disaster assessment, and other fields [7].

However, with the increase in the number of msUASs held by general public, the problem of disorderly flight is becoming increasingly serious, and the corresponding flight safety problem of civil msUASs is gaining prominence [2]. Incidents of msUAS flight affecting the take-off and landing safety of civil aviation aircraft and threatening the security of important areas and facilities occur from time to time. To reduce the existing or potential security problems of civil msUASs to other facilities and areas, the control technology of msUASs has emerged and has been widely used [8].

An anti micro and small Unmanned Aircraft System (AmsUAS) is a radio technology for civilian msUAS control [9], which is closely related to the msUAS radio communication system. The common AmsUAS [10] is mainly the radio-based msUAS control technology, which achieves control by blocking the communication link of the msUAS, thus hindering its normal operation and forcing landing. According to the Report ITU-R M.2171 [11], the communication links of civil msUASs generally include the uplink remote control link, downlink information transmission link, telemetry link, and satellite links such as GPS, Beidou, and GLONASS used for navigation. Therefore, in general, the AmsUAS aims to block one or more of the above communication links to divert or force the landing of civil msUASs to realize the control of civil msUASs.

However, in the process of controlling the radio links of msUASs, high-power signal suppression is usually adopted, which causes interference not only to the communication link of msUASs but also to other radio systems that use the same frequency band or adjacent frequency band, such as the GPS altitude measuring equipment on aircraft, GPS positioning equipment of mobile communication base stations, and the uplink and downlink of mobile communication systems. The civil GPS signal is the spread spectrum signal with a frequency of 1575 MHz, a bandwidth of 2.046 MHz, and a spread spectrum gain of 43 dB [12]. The high spread spectrum gain of the GPS signal results in poor performance of some frequency band interference of the AmsUAS. Therefore, the AmsUAS will normally control the uplink remote control link and downlink information transmission link of msUASs.

In general, the msUAS is easier for controllers to find than the UA control station (UACS), and the radio transmission conditions between the controller and the msUAS are better. Therefore, it is easier to control the msUAS by suppressing its uplink. According to the report ITU-R M.2237 [13] and the frequency division of ITU region 3, as well as the frequency usage of the existing civil msUASs, the operating frequency of the uplink remote link of msUASs is 840.5–845.0 MHz. In the process of controlling this link, harmful interference will be generated to the code division multiple access (CDMA) mobile communication system in adjacent frequency bands.

Therefore, this paper aims to conduct interference analysis and determine the minimum frequency and distance intervals required for both AmsUAS and CDMA systems to coexist. Thus, the study aims to prevent the high-power repressive interference generated by the AmsUAS from affecting the uplink of CDMA.

The rest of this paper is organized as follows. The system model is presented in Sect. 2, and the proposed interference analysis of AmsUAS and CDMA system is presented in Sect. 3. Section 4 presents numerical examples to verify the derived result. Finally in Sect. 5 we conclude the main results of this paper.

## 2 System Model

We consider the interference between the AmsUAS and CDMA system as shown in Fig. 1, where the AmsUAS operates in the adjacent frequency band of CDMA. The msUAS comprises a msUA and a UACS, which is a type of remote control equipment and usually fixed on the ground or handheld. The CDMA system is equipped with a base station and mobile terminals. The AmsUAS controls the msUAS by high-power noise interference on the uplink remote control link. In Fig. 1, Line 1 is the control link of the AmsUAS to the msUAS, Line 2 is the interference link of the AmsUAS to the uplink of the CDMA system, and Line 3 and Line 4 are the communication links of the msUAS and CDMA systems, respectively.

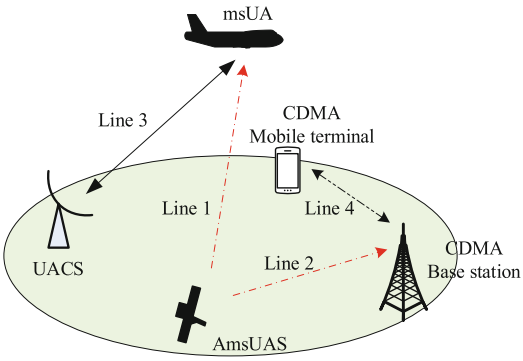


**Fig. 1.** System model

## 3 Interference Analysis of AmsUAS and CDMA System

Wireless interference always exists in the radio system [14–15]. The power of the interference signal is closely related to the distance between the transmitter and the receiver. As the distance increases, the interference signal decreases. Whether one radio system is harmful to another is assessed by interference analysis, which is usually based on a simple relationship [16–17]. A jamming signal with power within the allowable range of the receiver will generally not cause harmful interference to the receiver [12]. In this paper, interference analysis of a wireless communication system is performed based on the interference-to-noise ratio (INR) criterion to determine the ranges of frequency and distance separation for the two systems to coexist in time, frequency, and space domains [18].

### 3.1 Interference-To-Noise Ratio Criterion

Due to msUASs generally use frequency hopping and spread spectrum technology, and frequency hopping parameters can be self-adaptive, they have a certain ability of anti-jamming. In general, the controller does not know any other parameters other than the frequency band of the msUASs, so a high-power noise can only be used for full frequency band coverage.

When the AmsUAS controls the uplink of the msUASs, the power of the noise must be increased such that it exceeds the INR protection requirements of the msUASs, thereby allowing it to block the control of the UACS over the msUASs. According to report ITU-R M.2119 [19], the long-term protection requirement for an msUAS is −3 dB and the short-term protection requirement is 0 dB. To avoid harmful interference to the CDMA system of an adjacent channel, the power of the interference signal received by the CDMA base station must meet the INR protection requirements of normal communication. The INR protection requirement for the CDMA base station is $\eta_{CDMA} < -7$dB. INR is defined as

$$\mathrm{INR} = \frac{I}{N}, \tag{1}$$

where $I$ and $N$ denote the interference and noise power in W, respectively. The units of power can be converted into dB as $INR(\mathrm{dB}) = I - N$. The INR criterion can be defined as

$$\mathrm{INR} = \begin{cases} I_{msUAS} - N_{msUAS} \geq \eta_{msUAS} & \text{msUAS} \\ I_{CDMA} - N_{CDMA} < \eta_{CDMA} & \text{CDMA} \end{cases}, \tag{2}$$

where $I_{msUAS}$ and $N_{msUAS}$ are the interference and noise power received by the msUAS receiver, respectively. $\eta_{\mathrm{msUAS}}$ is the msUAS's INR protection requirement. For the AmsUAS to block the msUAS communication system, the requirement $INR \geq \eta_{\mathrm{msUAS}}$ must be met. $I_{CDMA}$ and $N_{CDMA}$ are, respectively, the interference and noise power received by the CDMA system. To ensure the normal quality of service, the requirement $INR < \eta_{\mathrm{CDMA}}$ must be met.

### 3.2 Calculation of Interference Power

In case of either the msUA or CDMA base station, the received interference power is a function of the gain and path loss. The interference power received by the jammed radio receiver is expressed by

$$I = P_{\mathrm{t}} + G_{\mathrm{t}} - L_{\mathrm{t}} + G_{\mathrm{r}} - L_{\mathrm{r}} - L_{\mathrm{p}}(d) - FDR(\Delta f). \tag{3}$$

Here, $P_{\mathrm{t}}$ is the transmit power of the interference source (dBm); $G_{\mathrm{t}}$ and $G_{\mathrm{r}}$ are the antenna gain of the transmitter and the receiver, respectively; $L_{\mathrm{t}}$ and $L_{\mathrm{r}}$ are the feeder loss of the AmsUAS and CDMA, respectively; and $L_{\mathrm{p}}(d)$ is the transmission path loss for a separation distance $d$ between the interferer and receiver (dB). $FDR(\Delta f)$ is a frequency-dependent rejection of a certain frequency separation $\Delta f$ (dB), which is a measure of the

rejection produced by the receiver selectivity curve on an unwanted transmitter emission spectra, defined as

$$FDR(\Delta f) = -10\log\frac{\int_{-\infty}^{+\infty} P(f)|H(f+\Delta f)|^2 df}{\int_{-\infty}^{+\infty} P(f)df} \quad \text{dB}. \tag{4}$$

Here, $P(f)$ is the power spectral density of the interfering signal equivalent intermediate frequency (IF); $H(f)$ is the frequency response of the receiver; $\Delta f$ is the frequency separation between jammed receivers and interfering transmitters, defined as $\Delta f = f_t - f_r$, where $f_t$ is the interferer-tuned frequency and $f_r$ is the receiver-tuned frequency. In particular, $\Delta f = 0$ indicates co-channel interference.

As can be seen from (4), the interference signal power is $P_\mathrm{t} = \int_{-\infty}^{+\infty} P(f)df$, $|H(f+\Delta f)|^2$ reflects the characteristics of the receiver spectrum mask, and $FDR(\Delta f) \geq 0$.

It is evident from (4) that $FDR(\Delta f)$ is strongly dependent on the extent of overlapping between the receiver passband and the power spectrum of the interfering signal. As $\Delta f$ increases, the extent of overlapping diminishes, thus resulting in lower interference power, and, equivalently, higher $FDR(\Delta f)$.

Considering the effect of the off-axis angle on the antenna gain, the off-axis angle of the transmitting antenna is defined as $\theta_1$ and that of the receiving antenna is defined as $\theta_2$. Then the interference power is

$$I = P_\mathrm{t} + G_\mathrm{t}(\theta_1) - L_\mathrm{t} + G_\mathrm{r}(\theta_2) - L_\mathrm{r} - L_\mathrm{p}(d) - FDR(\Delta f), \tag{5}$$

where, $G_\mathrm{t}(\theta_1)$ is the antenna gain of the AmsUAS in the direction of the receiver when the off-axis angle is $\theta_1$ (dBi); $G_\mathrm{r}(\theta_2)$ is the antenna gain of the jammed receiver (e.g., msUAS) in the direction of interference when the off-axis angle is $\theta_2$ (dBi).

According to the calculation method of a 100 MHz–70 GHz antenna radiation pattern given in ITU-R F.699–7 and ITU-R F.1245–1 recommendations, $D$ is the diameter or length of the antenna and $\lambda$ is the wavelength, $G_{max}$ is the maximum gain for the antenna and $G_1$ is the first side lobe gain, and $\theta_{3dB}$ is a 3 dB beam width. Then, the antenna gain $G_\Lambda(\theta_i)(\Lambda = \mathrm{t,r};\ i = 1, 2, 3)$ corresponding to different off-axis angles $\theta_i$ is given as follows.

When $D/\lambda > 100$,

$$G_\Lambda(\theta_i) = \begin{cases} G_\mathrm{max} - 2.5 \times 10^{-3}(D\theta_i/\lambda)^2, & 0^\circ < \theta_i < \varphi_m \\ G_1, & \varphi_m \leq \theta_i < \max(\varphi_m, \varphi_r) \\ 29 - 25\log\theta_i, & \max(\varphi_m, \varphi_r) \leq \theta_i < 48^\circ \\ -13, & 48^\circ \leq \theta_i \leq 180^\circ \end{cases} \tag{6}$$

where $G_\mathrm{max} = 20\log(D/\lambda) + 7.7$, $\varphi_m = \left(20D\sqrt{G_\mathrm{max} - G_1}\right)/\lambda$, $G_1 = 2 + 15\log(D/\lambda)$ and $\varphi_r = 12.02(D/\lambda)^{-0.6}$.

When D/λ ≤ 100,

$$G_\Lambda(\theta_i) = \begin{cases} G_{\max} - 2.5 \times 10^{-3}(D\theta_i/\lambda), & 0^\circ < \theta_i < \varphi_m \\ 39 - 5\log(D/\lambda) - 25\log\theta_i, & \varphi_m \le \theta_i < 48^\circ \\ -3 - 5\log(D/\lambda), & 48^\circ \le \theta_i \le 180^\circ \end{cases}. \tag{7}$$

### 3.3 Calculation of Path Loss

A spatial factor is used in the computation of distance-related signal attenuation; it is closely related to the radio propagation model adopted in this study and the statistical distribution of the interfering signal at the front end of the interfered receiver [22].

Path loss is calculated by radio propagation models. In this study, a radio propagation model is selected according to the system configuration, system bandwidth, operating frequency band, and geographical environment surrounding the service area [23].

Considering that the AmsUAS generally uses high-power signal suppression, in order to minimize its effect on other surrounding radio services, directional antenna is used for jamming the msUAS. To attain the minimum interference power of the AmsUAS, the free-space radio propagation model is used to calculate the path loss by the following formula:

$$L_{\mathrm{p}}(d) = 32.4 + 20\log d + 20\log f. \tag{8}$$

In the interference analysis of the AmsUAS and CDMA systems, path loss calculation methods of urban, suburban, or open scenarios in the Okumura–Hata model are adopted according to different application scenarios. The formulas of path loss in the three scenarios are as follows.

Radio propagation model in the urban scenario:

$$L_{\mathrm{p}}(d) = 49.55 + 26.16\lg f - 13.82\lg h_1 - \alpha(h_2) + (44.9 - 6.55\lg h_1)\lg d, \tag{9}$$

Where $f$ is the operating frequency; $h_1$ is the effective height of the base station antenna (m); $h_2$ is the effective height of the mobile station antenna (m); and $\alpha(h_2)$ is the height factor of the mobile station antenna (dB), and when $f > 400$ MHz, it is defined as

$$\alpha(h_2) = 3.2\left[\log(11.75h_2)\right]^2 - 4.97 \ (f > 400\,\mathrm{MHz}). \tag{10}$$

Radio propagation model in the suburban scenario:

$$L_{\mathrm{p}}(d) = 69.55 + 26.16\log f - 13.82\log h_1 - \alpha(h_2) + (44.9 - 6.55\log h_1)\log d. \tag{11}$$

For the suburbs scenario, $\alpha(h_2)$ is defined as

$$\alpha(h_2) = 2\left[\log(f/28)\right]^2 + 5.4. \tag{12}$$

Radio propagation model in the open scenario:

$$\begin{aligned} L_p(d) &= 28.6 + 26.16\log f - 13.82\log H_{\mathrm{b}} \\ &+\left[44.9 - 6.55\log(H_{\mathrm{b}})\right]\log d - 4.78(\log f)^2 + 18.33\log f, \end{aligned} \tag{13}$$

where $H_{\mathrm{b}}$ is the base station height.

### 3.4 Calculation of Minimum Interference Power

The transmit power of the AmsUAS is closely related to the transmit power, bandwidth, antenna gain, and anti-interference threshold of the receiver of the msUA. In practice, the maximum power received by the receiver is

$$P_{r\_\max} = \max\left\{P_{\mathrm{t}} + G_{\mathrm{t}}(\theta_1) - L_{\mathrm{t}} + G_{\mathrm{r}}(\theta_2) - L_{\mathrm{r}} - L_{\mathrm{p}}(d_1)\right\}, \tag{14}$$

where $P_{r\_\max}$ is the maximum power received by the msUA and $d_1$ is the propagation distance between the UACS and msUA.

To realize the effective interference of the AmsUAS to the msUAS uplink, the following inequation must be satisfied:

$$P_{t\_AmsUAS} + G_{\mathrm{t}}(\theta_1) - L_{\mathrm{t}} + G_{\mathrm{r}}(\theta_2) - L_{\mathrm{r}} - L_{\mathrm{p}}(d_2) - Th_{msUAS} \geq P_{r\_\max}, \tag{15}$$

where $P_{t\_AmsUAS}$ is the transmit power of the AmsUAS, $Th_{msUAS}$ is the anti-jamming threshold of the msUA, $d_2$ is the propagation distance between the AmsUAS and msUA. In general, $d_2$ is greater than $d_1$.

Suppose the UACS and AmsUAS have the same $G_{\mathrm{t}}(\theta_1)$ and $L_{\mathrm{t}}$, then for a given $d_2$, the interference power must satisfy

$$P_{t\_AmsUAS} \geq P_{r\_\max} - G_{\mathrm{t}}(\theta_1) + L_{\mathrm{t}} - G_{\mathrm{r}}(\theta_2) + L_{\mathrm{r}} + L_{\mathrm{p}}(d_2) + Th_{msUAS}. \tag{16}$$

### 3.5 Interference Analysis

With the high-power noise emitted by the AmsUAS, not only does the bottom noise in the surrounding airspace greatly increase but the main and side lobes of the antenna also cause interference to other nearby radio services, thus seriously affecting their normal operation.

The interference power received by the disturbed receiver is closely related to the operating frequency of the transmitted signal, the transmit power, and the distance between the transmitter and the receiver [25]. According to the INR criterion, measures that should be taken to avoid harmful interference include increasing the frequency separation, reducing the transmit power, increasing off-axis angles, or increasing the distance between transmitters and disturbed receivers [26, 27].

According to (2) and (5), when the AmsUAS generates interference, the receiver of adjacent frequency bands can only work normally when the following equation is satisfied.

$$I - N = P_{t\_AmsUAS} + G_{\mathrm{t}}(\theta_1) - L_{\mathrm{t}} + G_{\mathrm{r}}(\theta_3) - L_{\mathrm{r}} - L_{\mathrm{p}}(d_3) - FDR(\Delta f) - N_{CDMA} < \eta_{CDMA} \tag{17}$$

Where, $d_3$ is the propagation distance between AmsUAS and CDMA. $G_{\mathrm{r}}(\theta_3)$ is the antenna gain of the jammed receiver (e.g. CDMA) in the direction of interference when the off-axis angle is $\theta_3$. $N_{CDMA}$ is mainly generated by the thermal motion of charged particles, and its power is.

$$N_{CDMA} = -174 + 10\log B + NF\ dBm, \tag{18}$$

where $B$ is the medium frequency bandwidth (Hz) and $NF$ denotes the noise figure (dB).

In case when the radio wave propagation distance $d_3$ is given, the relationship between the transmit power of the AmsUAS and frequency separation can be obtained as follows.

$$P_{t\_AmsUAS} < \eta_{CDMA} - G_{\mathrm{t}}(\theta_1) + L_{\mathrm{t}} - G_{\mathrm{r}}(\theta_3) + L_{\mathrm{r}} + L_{\mathrm{p}}(d_3) + FDR(\Delta f) + N_{CDMA} \tag{19}$$

Then, the maximum transmitting power is $P_{t\_\max} = \max\{P_{t\_AmsUAS}\}$. As can be seen from (14), $P_{t\_AmsUAS} \in [P_{t\_\min}, P_{t\_\max}]$.

In case $P_{t\_AmsUAS}$ is given, according to (17), the frequency and distance separation between the AmsUAS and CDMA systems can be obtained as follows.

$$\begin{aligned} 20\log(d_3) \geq\ & P_{t\_AmsUAS} + G_{\mathrm{t}}(\theta_1) - L_{\mathrm{t}} + G_{\mathrm{r}}(\theta_3) - L_{\mathrm{r}} \\ & - FDR(\Delta f) - N_{CDMA} - 32.4 - 20\log f - \eta_{CDMA} \end{aligned} \tag{20}$$

## 4 Numeric Simulation and Discussion

In this section, we present the simulation results to verify the proposed interference analysis method. The simulation scenario includes an msUA, a UACS, an AmsUAS, and a CDMA base station. DQPSK modulated signals are transmitted by the msUAS. The flight altitude of the msUAS is less than 1000 m, and the simulation parameters of the msUAS are shown in Table 1.

**Table 1.** Simulation parameters of msUAS.

| | Bandwidth (MHz) | Transmit power (dBm) | Antenna gain (dBi) | Antenna height (m) | Feeder loss (dB) | NF (dB) | INR Requirements (dB) |
|---|---|---|---|---|---|---|---|
| Transmitter | 50 | 33 | 20 | 1.5 | 2 | 5 | / |
| Receiver | 50 | / | 3 | <1000 | 1 | 5 | −3 |

To determine the maximum power received by the msUAS, as the propagation model of the msUAS, the free space model is used to calculate the path loss. Figure 2 shows the signal power received by the msUA at different propagation distances and receiving off-axis angles.

When $\theta_2 = 0^{\circ}$, there is no off-axis angle between the receiving antenna and the main beam direction of the UACS. $\theta_2 \neq 0^{\circ}$ indicates that the receiving antenna deviates from the main beam direction at $\theta_2$. When $\theta_2 = 0^{\circ}$, the power of the received signal is maximum; the larger the off-axis angle, the smaller the received signal power. For a given transmit power, the greater the transmission distance, the smaller the received signal power.

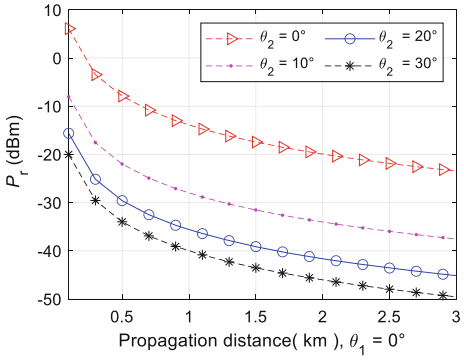


**Fig. 2.** Power of the received signal corresponding to different propagation distances, where $\theta_1 = 0^\circ$.

Figure 3 shows comparison of the minimum interference power of the AmsUAS for different propagation distances and off-axis angle $\theta_1$. To block the uplink communication system of the msUAS, the minimum noise interference signal power transmitted by the AmsUAS should be greater than or equal to the sum of the maximum received signal power and the anti-interference threshold of the msUAS. In general, when the main beam direction of the AmsUAS is directly opposite to the msUA, i.e., $\theta_1 = 0^\circ$, the transmitted power is the least. However, to avoid interference with other radio communication systems in the same direction, the main beam direction can be deviated from the msUA, i.e., $\theta_1 \neq 0^\circ$. A short communication link between the AmsUAS and msUA ensures less interference power, and thus a low possibility of interfering with other radio services. Considering the effect of path loss, the minimum interference power obtained by the free space radio propagation model is the least. With other radio propagation models, the minimum interference power will be larger.

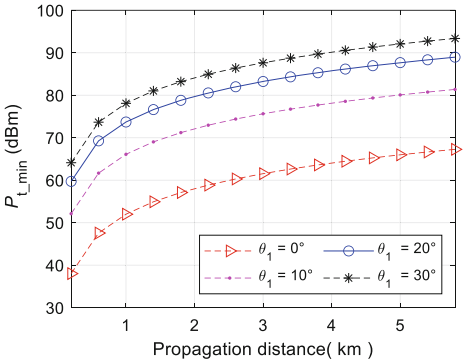


**Fig. 3.** Minimum interference power of the AmsUAS corresponding to different propagation distances.

A high-power noise-jamming signal transmitted by the AmsUAS will interfere with radio equipment located within a certain distance. To avoid harmful interference, the

AmsUAS and CDMA systems need to meet certain frequency and distance separation as mentioned in Subsect. 3.5. Figures 4 and 5 show frequency separation versus distance separation for different off-axis angles in an urban scenario. The simulation parameters of CDMA are shown in Table 2. The Okumura–Hata urban propagation model is used to calculate the path loss. When the main beam direction of the AmsUAS is directed toward the CDMA base station, i.e., $\theta_3 = 0^\circ$, a larger distance separation is required to ensure that the CDMA base station is not subject to harmful interference. Increasing the off-axis angle $\theta_3$ can also effectively reduce the distance separation. Comparison of Figs. 4 and 5 indicates that reducing the transmit power $P_{\text{t\_ min}}$ can also effectively reduce the distance separation. Therefore, in practical applications, the transmit power of the AmsUAS and off-axis angle should be reasonably selected.

**Table 2.** Simulation parameters of CDMA.

| | Bandwidth (MHz) | Antenna gain (dBi) | Antenna height (m) | Feeder loss (dB) | NF (dB) | INR requirments (dB) |
|---|---|---|---|---|---|---|
| Base station | 1.25 | 15 | 30 | 2 | 5 | −7 |

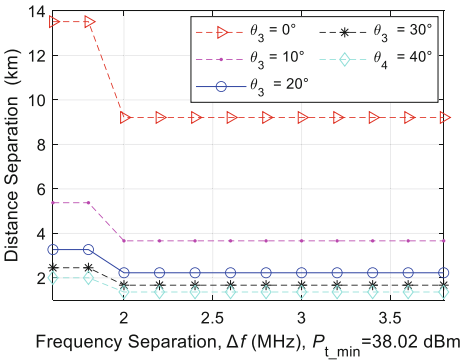


**Fig. 4.** Frequency separation with respect to distance separation under different off-axis angles in an urban scenario with $P_{\text{t\_ min}} = 38.02$ dBm.

According to the radio propagation theory, path loss is an important factor in the analysis of interference between different wireless communication systems. Figures 6 and 7 show frequency separation versus distance separation in suburban and open scenarios, respectively. Path loss is calculated using the Okumura–Hata suburban and the open environment propagation models, respectively. The figures indicate that the path loss of a suburban scenario is greater than that of an open scenario. Therefore, under the condition of the same frequency separation, the distance separation of an open scenario is greater than that of a suburban scenario. Therefore, in an open scenario, the power of the interference signal should be carefully selected to avoid harmful interference to other radio systems.

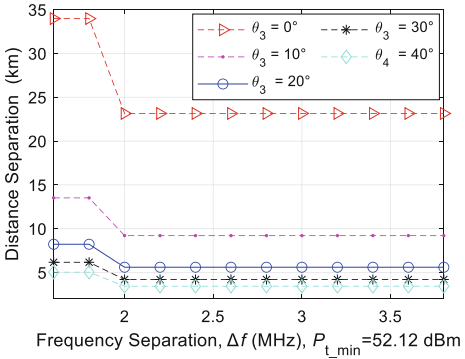


**Fig. 5.** Frequency separation with respect to distance separation under different off-axis angles in an urban scenario with $P_{\mathrm{t\_min}} = 52.12$ dBm.

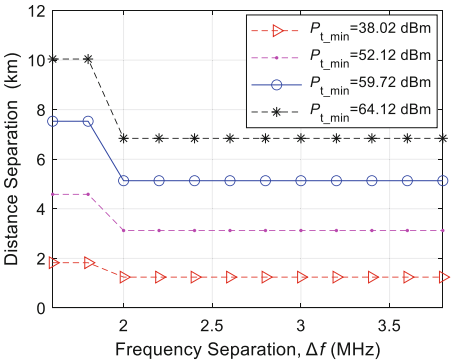


**Fig. 6.** Frequency separation with respect to distance separation under different $P_{\mathrm{t\_min}}$ in a suburban scenario

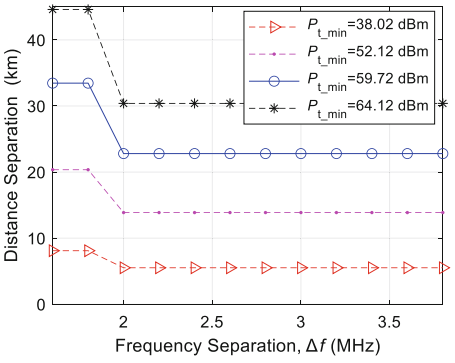


**Fig. 7.** Frequency separation with respect to distance separation under different $P_{\mathrm{t\_min}}$ in an open scenario

## 5 Conclusions

In practice, the AmsUAS not only interferes with msUAS communication links but also can cause harmful interference to civil aviation and mobile communication systems. This study analyzed the radio interference of the AmsUAS and CDMA. First, the minimum transmit power of the AmsUAS in the corresponding frequency band was calculated on the basis of the parameters of the controlled msUA and the wave propagation distance. Second, according to the working frequency band, application scenario, and distance between AmsUAS and CDMA base stations, interference analysis was performed on the basis of the INR criterion to obtain the frequency and distance separation that must be satisfied for both systems to coexist. Finally, the simulation verified the feasibility and effectiveness of the proposed method.

**Author Contributions.** J. Li conceived and designed the experiments; C. Zhang and J. Liu performed the experiments; J. Li,Y. Zhang and K. Liu analyzed the data; J. Li, K. Liu and F. Song wrote the paper. All authors have read and agreed to the published version of the manuscript.

**Funding.** This work was supported in part by the Aeronautical Science Foundation under Grant No. 2019ZH0T7001 and in part by the Scientific Research Foundation of Xi'an Aeronautical University under Grant No. 2019KY0207.

**Conflicts of Interest.** The authors declare no conflict of interest.

## References

1. Papa, U.: Introduction to Unmanned Aircraft Systems (UAS). Embedded Platforms for UAS Landing Path and Obstacle Detection, January 2018
2. Lieb, T.J., Volkert, A.: Unmanned aircraft systems traffic management: a comparison on the FAA UTM and the European CORUS ConOps based on U-space. In: 39th Digital Avionics Systems Conference (DASC), San Antonio, TX, USA, pp.1–6 (2020)
3. Karaca, Y., Cicek, M., et al.: The potential use of unmanned aircraft systems (drones) in mountain search and rescue operations. Am. J. Emergency Med. **36**(4), 583–588 (2018)
4. Grubinger, S., et al.: Modeling realized gains in Douglas-fir (Pseudotsuga menziesii) using laser scanning data from unmanned aircraft systems (UAS). Forest Ecol. Manage. **473** (2020). https://doi.org/10.1016/j.foreco.2020.118284
5. Adkins, K., Wambolt, P., Sescu, A., Swinford, C., et al.: Observational practices for urban microclimates using meteorologically instrumented unmanned aircraft systems. Atmosphere (11) (2020). https://doi.org/10.3390/atmos11091008
6. Gaston, M.D., et al.: Customizing unmanned aircraft systems to reduce forest inventory costs: can oblique images substantially improve the 3D reconstruction of the canopy? Int. J. Remote Sens. **41**(9), 3480–3510 (2020)
7. Cunningham, M., et al.: Aeromagnetic surveying with a rotary-wing unmanned aircraft system: a case study from a zinc deposit in Nash Creek, New Brunswick, Canada. Pure Appl. Geophys. **175**(9), 3145–3158 (2018)
8. Jie, L., Chaofeng, L., Cheng, D., Tong, F., Nimin, Z., Hang, Z.: Necessity analysis and scheme of constructing ultra-low-altitude defense system in megacities. IEEE Aerosp. Electron. Syst. Mag. **36**(1), 14–21 (2021)

9. Xufang, S., Chaoqun, Y., Weige, X., Liang, C., Shi, Z., Chen, J.: Anti-drone system with multiple surveillance technologies: architecture implementation and challenges. IEEE Commun. Mag. **56**(4), 68–74 (2018)
10. Daojing, H., et al.: A friendly and low-cost technique for capturing non-cooperative civilian unmanned aerial vehicles. IEEE Network **33**(2), 146–151 (2019)
11. International Telecommunication Union Radiocommunication Study Group. Characteristics of unmanned aircraft systems and spectrum requirements to support their safe operation in non-segregated airspace (Report ITU-R M.2171). International Telecommunication Union Publications 2009 (2009)
12. Oh, M., Kim, Y.H.: Statistical approach to spectrogram analysis for radio-frequency interference detection and mitigation in an l-band microwave radiometer. Sensors **19**, 306 (2019). https://doi.org/10.3390/s19020306
13. International Telecommunication Union Radiocommunication Study Group. Compatibility study to support the line-of-sight control and non-payload communications link(s) for unmanned aircraft systems proposed in the frequency band 5 030–5 091 MHz (Report ITU-R M.2237). International Telecommunication Union Publications 2011
14. Biswas, S., Singh, K., Taghizadeh, O., Ratnarajah, T.: Coexistence of MIMO radar and FD MIMO cellular systems with QoS considerations. IEEE Trans. Wireless Commun. **17**(11), 7281–7294 (2018)
15. Chen, H., Hua, J., Li, F., Chen, F., Wang, D.: Interference analysis in the asynchronous f-OFDM systems. IEEE Trans. Commun. **67**(5), 3580–3596 (2019). https://doi.org/10.1109/TCOMM.2019.2898867
16. Biswas, S., Singh, K., Taghizadeh, O., Ratnarajah, T.: Design and analysis of FD MIMO cellular systems in coexistence with MIMO radar. IEEE Trans. Wireless Commun. **19**(7), 4727–4743 (2020)
17. Prasan, S., Sudhir, P., Shih-Lin, W.: A reliable data transmission model for IEEE 802.15.4e enabled wireless sensor network under WiFi interference. Sensors **17**(6), 1320 (2017). https://doi.org/10.3390/s17061320
18. International Telecommunication Union Radiocommunication Study Group. Recommendation ITU-R SM.337–6 Frequency and distance separations. International Telecommunication Union Publications 2008
19. International Telecommunication Union Radiocommunication Study Group. Sharing between aeronautical mobile telemetry systems for flight testing and other systems operating in the 4400–4940 and 5925–6700 MHz bands (Report ITU-R M.2119). International Telecommunication Union Publications 2007
20. International Telecommunication Union Radiocommunication Study Group. Reference radiation patterns for fixed wireless system antennas for use in coordination studies and interference assessment in the frequency range from 100 MHz to 86 GHz. International Telecommunication Union Publications 2018
21. International Telecommunication Union Radiocommunication Study Group. Mathematical model of average and related radiation patterns for line-of-sight point-to-point radio-relay system antennas for use in certain coordination studies and interference assessment in the frequency range from 1 GHz to about 70 GHz, Recommendation ITU-R F.1245–1. International Telecommunication Union Publications 2000
22. International Telecommunication Union Radiocommunication Study Group. Propagation curves for aeronautical mobile and radionavigation services using the VHF, UHF and SHF bands (ITU-R P.528–2). International Telecommunication Union Publications 1986
23. Raymond, S., Abubakari, A., Jo, H.-S.: Coexistence of power-controlled cellular networks with rotating radar. IEEE J. Sel. Areas Commun. **34**(10), 2605–2616 (2016)
24. Andersen, J.B., Rappaport, T.S., Yoshida, S.: Propagation measurements and models for wireless communications channels. IEEE Commun. Mag. **33**(1), 42–49 (1995)

25. Khawar, A., Abdelhadi, A., Clancy, T.C.: Coexistence analysis between radar and cellular system in LoS channel. IEEE Antennas Wireless Propag. Lett. **15**, 972–975 (2016)
26. Yusra, B., Rather, G.M., Begh, G.R.: SINR analysis and interference management of macrocell cellular networks in dense urban environments. Wireless Personal Commun. **111**(9), 1645–1665 (2020)
27. Polak, L., Milos, J.: Performance analysis of LoRa in the 2.4 GHz ISM band: coexistence issues with Wi-Fi. Telecommun. Syst. Model. Anal. Des. Manage. **74**(3), 299–309 (2020)